Journal of Magnetism and Magnetic Materials 500 (2020) 166261

Contents lists available at ScienceDirect

Journal of Magnetism and Magnetic Materials

journal homepage: www.elsevier.com/locate/jmmm

Research articles

Existence of exchange bias and Griffith phase in $(Tb_{1-x}Ce_x)MnO_3$

Surajit Ghosh[a], Abhishek Kumar[a,1], Arkadeb Pal[a], Prajyoti Singh[a], Prince Gupta[a], Khyati Anand[a], U.K. Gautam[b], A.K. Ghosh[c], Sandip Chatterjee[a,*]

[a] Department of Physics, Indian Institute of Technology (BHU), Varanasi 221005, India
[b] Raja Ramanna Centre for Advanced Technology, Indore 452013, India
[c] Department of Physics, Banaras Hindu University, Varanasi 221005, India

A B S T R A C T

The structural and magnetic properties of $(Tb_{1-x}Ce_x)MnO_3$ have been investigated. The presence of Griffith's phase has been confirmed from the AC susceptibility study of the materials. The observed Griffith phase in $(Tb_{1-x}Ce_x)MnO_3$ is attributed to the exchange interaction between Mn^{3+}/Mn^{2+} ions. Chemical analysis by X-ray photo-emission spectroscopy has shown the presence of mix valence state of Mn and oxygen vacancy in the materials. At low temperatures, the materials also show existence of exchange bias in field cooled condition which changes with Ce content. Jahn-Teller distortion and oxygen vacancy are found to dominate in these systems to change the Mn–O–Mn bond angle which in turn induce canted antiferromagnetism (AFM) in this system. The canted AFM plays an important role in getting the exchange bias effect.

1. Introduction

In recent years, multifunctional materials have attracted valuable interest due to the coexistence of more than two properties simultaneously in one material e.g. multiferroicity, exchange Bias (anisotropy in hysteresis loop), Griffiths phase (inhomogeneity in spin ordering) etc. [1–5]. Many intrinsic multifunctional materials have been discovered and many artificially created by mixing two or more than two materials (like composites) or substituting some species of parent compound. Thus, the study of $RMnO_3$ (R = Gd, Tb, Dy, Ho) has gained considerable interest owing to the co-existence of magnetic ordering and ferroelectricity with a strong coupling between them [1–5]. In these systems, Jahn-Teller (JT) effect is found to be dominant due to presence of JT active Mn^{3+} ions which essentially produces structural disorder through bending of Mn–O–Mn bond angles and deformation of Mn–O bond lengths [1–5]. Critical physical processes and disordered magnetic states can evolve in the system due to the structural disorder. A decrease in ionic radius of the R enhances the competition in magnetic interactions, i.e. ferromagnetic between nearest neighbour Mn sites and anti-ferromagnetic between next nearest neighbour sites [6]. $TbMnO_3$, a widely studied material of current times owes its interest to the strong magnetoelectric coupling as it lies in the intermediate coupling region [2,7–14]. The material shows ferroelectricity below 27 K and two antiferromagnetic (AFM) ordering i.e., Mn^{3+} magnetic moments order ~41 K (T_{N1}) while Tb^{3+} magnetic moments order ~10 K (T_{N2}) [3]. The frustrated spiral spin order of Mn^{3+} in $TbMnO_3$ is thought to be the origin of ferroelectricity making it a type-II multiferroic material [15]. The system in the intermediate coupling regime is very sensitive to any variation in J_{Mn-R} (exchange interaction between manganese and rare-earth ions) which strongly affects the Tb-magnetic ordering as has been observed by Prokhnenko et al., [16].

The phenomenon of exchange anisotropy or bias (EB) is typically associated with a shifting of the hysteresis loop (Exchange-bias field, H_E), measured after field-cooling (spontaneous) or zero field cooling (conventional) of a ferromagnetic (FM)-AFM interface through the Néel temperature T_N of the AFM component [17,18]. EB effect can found to be applicable in the development of permanent magnets, magnetic recording media or domain stabilizers in recording heads based on anisotropic magnetoresistance. In exchange biased systems, reduced value of saturation field as well as giant magnetoresistance (GMR) can be found simultaneously as compared to standard GMR multilayer systems, which triggered a renewed interest in these phenomena. Furthermore, the observation of a Griffith's phase (GP) in a number of doped Perovskite manganite oxides has gained much interest over the years. According to Griffith's theory, there is always a finite probability of finding ferromagnetic (FM) clusters with randomly distributed spin [i.e., in paramagnetic (PM) state] in the temperature range $T_C < T < T_G$ (where, T_C is the Curie-Weiss temperature and T_G is the Griffith's temperature which marks the onset of completely random magnetic interactions) [19]. The Griffith phase is understood by the formation of FM clusters above the long range ordering temperature (T_C or T_N) and below T_G which are formed thermodynamically during

* Corresponding author.
E-mail address: schatterji.app@iitbhu.ac.in (S. Chatterjee).
[1] Present address: Indian Institute of Geomagnetism, New Panvel, Navi Mumbai, India.

https://doi.org/10.1016/j.jmmm.2019.166261
Received 17 April 2019; Received in revised form 11 November 2019; Accepted 1 December 2019
Available online 10 December 2019
0304-8853/

cooling and nucleated by the intrinsic randomness. This causes inhomogeneous magnetic distribution in the sample which makes the magnetization of the materials to be anon-analytic function of the magnetic fields. Nevertheless, Griffith phase can be characterized by the downturn deviation from Curie-Weiss law behavior in χ^{-1} as the temperature approaches to T_C from above [20].

So far no report is available regarding the existence of Griffith phase and exchange bias in $TbMnO_3$. Rubi et al. have shown the ferromagnetic like interaction below the bulk Neel temperaturein $TbMnO_3$ thin film [21]. They have proposed the coupling between magnetization and strain as the origin of ferromagnetism. Recently, O'Flynn et al. have reported the bifurcation between ZFC and FC magnetization in $TbMnO_3$ single crystal [22]. In an earlier report Kumar et al, have observed indication of Griffith phase in these systems [23]. In this paper, we report the existence of both exchange bias and Griffith phase in $Tb_{1-x}Ce_xMnO_3$ (0, 0.025, 0.05) and also discuss the enhancement of Griffith phase with hole doping (by doping Ce) in $TbMnO_3$. The observations have been analyzed and understood from formation or mix valence states due to oxygen vacancy and canted antiferromagnetism due to JT distortion present in the system.

2. Experimental detail

The $Tb_{1-x}Ce_xMnO_3$ (x = 0.0, 0.025, 0.05) polycrystalline samples were synthesized by the conventional solid state reaction technique. Stoichiometric amounts of Tb_4O_7, MnO (99.99% purity) and CeO_2 were mixed and heated at 1000 ^{0}C for 12 h. The resulting powders were ground and pressed into pellets and sintered at 1200 ^{0}C for 24 h. The final step consisted on repressing and sintering the pellets at 1300 °C for 48 h with one intermediate grinding. Single phase of the samples was characterized by x-ray diffractometer (Model: MiniFlex II, Rigaku, Japan) with Cu Kα radiation (λ = 1.5406 Å). Magnetic Measurement was done by SQUID (PPMS) magnetometer (Quantum Design). The x-ray photoemission spectra were recorded at the Hard X-ray Photo-Electron Spectroscopy (HAXPES) beamline (PES-BL14), housed at the 1.5 T bending-magnet port at the Indian synchrotron (Indus-2), Indore, India.

3. Results and discussion

Fig. 1 shows of the XRD patterns of $Tb_{1-x}Ce_xMnO_3$ (x = 0.0, 0.025, 0.05) with Rietveld refinement. The refinement results clearly suggest the formation of single phase polycrystalline $TbMnO_3$ in orthorhombic structure with *Pbnm* space group. The detail crystallographic results are tabulated in Table 1 from which it can be seen that the parameters deviate from that of ideal *Pbnm* ones and the deviations are larger for $Tb_{0.975}Ce_{0.025}MnO_3$ than $Tb_{0.95}Ce_{0.05}MnO_3$. The bond angles between Mn-O1-Mn and Mn-O2-Mn present in the lattice have been estimated from the refinement results to find that the bond angle changes when the Ce is doped in $TbMnO_3$. The changes can be attributed to the presence of oxygen vacancies in the lattice and Jahn-Teller (JT) distortion of the MnO_6 octahedra due to presence of Mn^{3+} ions in the lattice. In fact, there are a few factors which affect the crystal structure of the materials like, the Jahn-Teller distortion, difference in ionic radii in Tb and Ce ions, and charge difference between constituent ions. It can also be seen that all the samples satisfy the condition for the JT distortion [b > a > c/√2]. The difference in the ionic radii between Tb^{3+}, Ce^{4+} which are 0.923 Å and 0.870 Å respectively in six-fold coordination, can also have its effect on the crystal parameters of the samples [24]. The introduction of Ce^{4+} ions in the lattice is expected to create mix valence of Mn ions to maintain the charge neutrality. Thus, the effective JT distortion will be reduced in Ce doped samples due to smaller number of JT active Mn^{3+} ions. In distortion free perovskite structure the Mn–O–Mn angle should be 180° which reduces to ~145° for the pure $TbMnO_3$ lattice due to large JT distortion. For $Tb_{0.975}Ce_{0.025}MnO_3$ the bond angle deviation from 180° reduces due to reduction in JT distortion. Further increase in the deviation of the bond angle in $Tb_{0.95}Ce_{0.05}MnO_3$ can be ascribed to the strain in the lattice created due to the difference between the ionic radii of Tb^{3+} and Ce^{4+}.

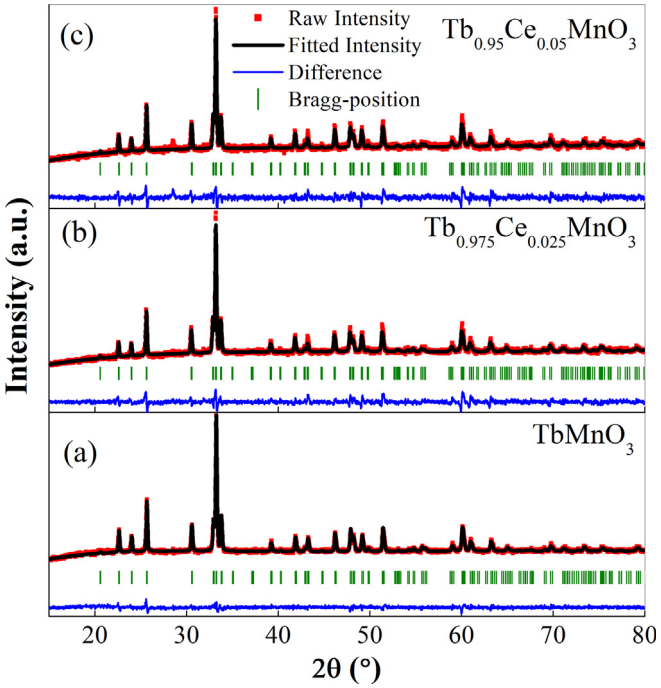

Fig. 1. (a, b, c) Reitveld refinement of XRD pattern of $TbMnO_3$, $Tb_{0.975}Ce_{0.025}MnO_3$ and $Tb_{0.95}Ce_{0.05}MnO_3$ respectively.

Table 1
Reitveld refined lattice parameter, Mn–O–Mn bond angle and Griffith temperature (T_G) and Curie Temp. (T_C) calculated by CW (Curie-Weis) fitting of inverse magnetic susceptibility vs Temperature of $TbMnO_3$, $Tb_{0.975}Ce_{0.025}MnO$ and, $Tb_{0.95}Ce_{0.05}MnO_3$.

Parameters	Sample		
	$TbMnO_3$	$Tb_{0.975}Ce_{0.25}MnO_3$	$Tb_{0.95}Ce_{0.05}MnO_3$
a (Å)	5.3029(2)	5.3112(3)	5.3096(3)
b (Å)	5.8458(2)	5.8570(3)	5.8503(4)
c (Å)	7.4094(2)	7.4192(4)	7.4195(4)
T_G (Griffith Temp.) K	54	60	64
T_C (Curie Temp.) K	−30.76	−29.87	−31.70
Mn–O_1–Mn (deg.)	144.4 (6)	158.0 (4)	151.6 (4)
Mn–O_2–Mn (deg.)	144.9 (5)	167.5 (5)	157.0 (4)

Fig. 2(a) shows the temperature variation of magnetization (M-T) measured in both zero field cooled (ZFC) and field cooled (FC) mode of pure $TbMnO_3$. A peak ~10 K can be seen in the M-T plot which refers to the ordering of Tb^{3+} ions commonly found in $TbMnO_3$ [17,22,23]. Fig. 2 (b-d) show the inverse susceptibility $1/\chi$ vs temperature (5–80 K) of $TbMnO_3$, $Tb_{0.975}Ce_{0.025}MnO_3$ and $Tb_{0.95}Ce_{0.05}MnO_3$ under different cooling field of 5 kOe, 10 kOe, 20 kOe, 30 kOe respectively, fitted with the Curie-Weiss law. As expected the dominant magnetic interaction is found to be antiferromagnetic as the high temperature tail gives negative extrapolated intercept at the temperature axis. From Fig. 2(b), it can be observed that while in the high temperature region above 54 K, the magnetization follows Curie-Weiss (CW) law, deviation from CW behavior can be observed below 54 K. Similar downturns can also be observed for the sample $Tb_{0.975}Ce_{0.025}MnO_3$ and $Tb_{0.95}Ce_{0.05}MnO_3$ at 60 and 64 K respectively [Fig. 2(c) and (d)] indicating existence of different magnetic phases below 54 K [25–27]. It can be attributed to the presence of Griffith phase which arises in the system due to the formation of FM cluster embedded in AFM and PM region as observed

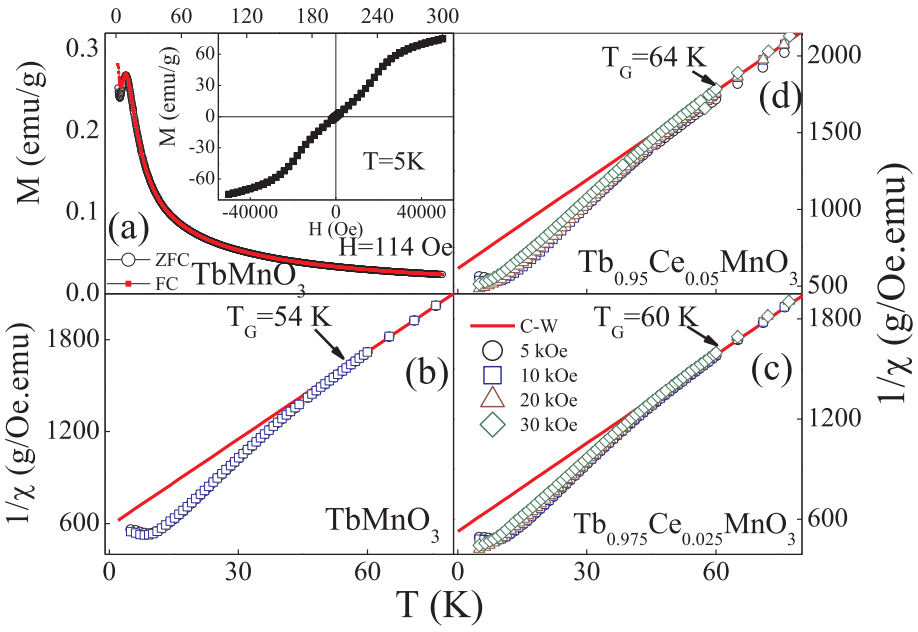

Fig. 2. (a, b, c) Curie-Weiss (CW) fitted curve of inverse susceptibility $1/\chi$ vs. temperature (5–80 K) of $TbMnO_3$, $Tb_{0.975}Ce_{0.025}MnO_3$ and $Tb_{0.95}Ce_{0.05}MnO_3$ underdifferent cooling field 5 kOe, 10 kOe, 20 kOe, 30 kOe respectively. (d) Magnetization vs Temperature of $TbMnO_3$ in the range of 2–300 K at 114 Oe (Inset shows M-H curve of $TbMnO_3$ at 5 K).

in inhomogeneous magnetic layers of different materials [28]. The observation of down-turn behaviour of $\chi^{-1}(T)$ at low fields is very crucial as it eventually helps one to distinguish the Griffiths phase from other non-Griffiths like clustered phases where $\chi^{-1}(T)$ deviates from CW law by showing an up-turn above ordering temperature [29]. The down-turn deviation gets softened with increasing magnetic fields and with sufficiently high magnetic fields the downturn vanishes, resembling perfect CW behaviour, which is also a hallmark for Griffiths phase [29]. Thus, the magnetization increases linearly with magnetic fields in paramagnetic regions and at high fields, PM susceptibility dominates over the contributions from the correlated clusters to the susceptibility. Moreover, it has been observed that the materials exhibiting GP usually give a larger effective spin S_{eff}, deduced from the slope of the Curie–Weiss fitting on the high-temperature magnetization, than the value for an effective Mn ion due to the contribution of individual entities containing more than two ions, i.e., FM clusters, in the high-temperature paramagnetic phase [27]. In our case, we evaluated the values of S_{eff} as 10.51μ_B, 10.9 μ_B and 10.41 μ_B for $TbMnO_3$, $Tb_{0.975}Ce_{0.025}MnO_3$ and $Tb_{0.95}Ce_{0.05}MnO_3$ respectively and we have also calculated these values theoretically as 10.88 μ_B, 10.77 μ_B and 10.66 μ_B respectively. It is observed that these values are very close to the S_{eff} calculated theoretically [20]. Moreover, the magnetic susceptibility of a material in Griffith's phase can be understood to be a sum the true paramagnetic (PM) susceptibility (χ_{PM}) and the susceptibility of the magnetically ordered clusters (χ_C). The value of χ_C is higher than χ_{PM} if the clusters are ferromagnetic. Thus the total susceptibility in the GP would exceed the value in the PM region resulting in the downturn in $\chi^{-1}(T)$ as one approaches T_C or T_N from the high temperature side. On the other hand, this condition of $\chi_C > \chi_{PM}$ may not hold if the clusters are antiferromagnetic (AFM). This is the reason for rarity of finding Griffith's phase in systems which shows PM to AFM transitions. However, there are few reports in which of existence of Griffith's phase has been observed in AFM ground state material where there are either mixed interactions or a FM ground state near the AFM state. In a recent report by Karmakar et al., GP was reported to be stabilized by the presence of short range FM superexchange interactions driven by structural distortions in the inherently AFM half-doped manganites [30].

The temperature dependence of the susceptibility in Griffith phase region is usually characterized as [19,31]

$$\chi^{-1}(T) \propto (T - T_C^R)^{1-\lambda} \quad (1)$$

where eq.1 is definitely a modified version of Curie Weiss law in which λ quantifies the presence of Griffiths phase. T_C^R stands for the critical temperature of random ferromagnetic clusters. More clusters achieve ordering as T_C or T_N is approached from above and as a result bulk susceptibility of the system tends to diverge at T_C^R (usually $>$ Tc or T_N) [32-34]. The fundamental role of T_C^R in attaining and modulating the GP is still not very clear despite several experimental researches till date. However, even if the sample does not attain long-range FM ordering, perhaps inter-cluster correlation of magnetic fluctuations develops. As a result of the formation of ferromagnetic clusters in the paramagnetic region deviation from the Curie Weiss behavior is expected which is reflected as the downturn in inverse susceptibility vs. temperature plot. Thus, T_C^R should be in between the actual ordering temperature and the highest ordering temperature allowed by the exchange bond interaction. The magnetic transition temperature (T_C or T_N) and T_C^R are reported to be very close for most of the compounds showing Griffith's phase [32,35,36]. We have used approximation in assigning the ordering temperature $T_C^R = T_N$ because our aim is to study the dependence of λ [30]. Fig. 3 shows a graph between $\log_{10}(T/T_N-1)$ vs $\log_{10}(\chi^{-1})$. At low temperature the data show another linear region just above T_N. This linear region fitted by the equation (1) which gives the non-zero value of λ, which lies in the range, $0 \leq \lambda < 1$. This value of λ confirms the existence of Griffith phase.

We have also studied the AC magnetization of doped and pure sample of $TbMnO_3$ to as the slow dynamics of the Griffith like phase, observed in DC magnetization, can be manifested in the frequency dependence of AC susceptibility also. AC susceptibility has been recorded as a function of temperature in the range (5–75) K under 5 Oe AC drive field at frequency 5, 50, 500 Hz and DC biasing field $H_{DC} = 0$, 10, 50 Oe. Fig. 4 shows the $1/\chi'$ (in phase) and χ'' (out of phase) vs T (temperature) of $TbMnO_3$ at different frequency under different DC biasing field 0 Oe, 10 Oe, 50 Oe respectively. The inverse of in phase susceptibility also shows deviations from the Curie–Weiss behaviour similar to the inverse DC susceptibility below 54 K. χ'' curve shows a significant increment in magnetic moment when the temperature is decreased below 54 K to Neel temperature 40 K (T_N) at higher frequency 500 Hz under biased field 50 Oe. The presence of non-zero component of AC susceptibility points out an energy loss process associated with domain dynamics which in turn indicates presence of other magnetic phases in the paramagnetic region. Although the domain dynamics process is usually conferred to a long range ordering, it can happen also in case of short-range ordering or weak ferromagnetism. Interestingly, the increment in moment is frequency

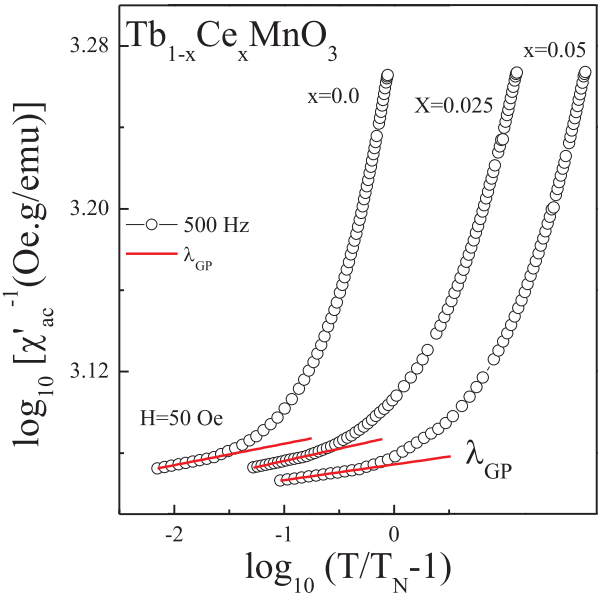

Fig. 3

Fig. 3. Temperature dependent susceptibility data of $Tb_{1-x}Ce_xMnO_3$ (x = 0.0, 0.025, 0.05), plotted in double logarithmic scale according to equation (1).

dependent and observed above ordering temperature (T_N) in high temperature PM phase. It might be due to the ferromagnetic clustering which is an evidence of Griffith phase as observed in DC magnetization analysis [37,38]. It can be conferred from the AC magnetization study that the FM clusters in the GP like state relaxes with a slow dynamics and it fluctuates in fast relaxation time. In doped sample x = 0.025 and 0.05 this increment in magnetic moment has also been observed with slight increment in Griffith temperature T_G = 60 K and 64 K respectively as shown in Figs. 5 and 6. Figs. 5 and 6 also show the deviation from CW behaviour of inverse of in-phase susceptibility (1/χ') confirming the presence of Griffith's phase below 60 and 64 K in $Tb_{0.975}Ce_{0.025}MnO_3$ and $Tb_{0.95}Ce_{0.05}MnO_3$ respectively. The enhancement of the Griffith phase temperature T_G with Ce doping has also been observed in the DC magnetization measurement. Both AC and DC magnetic susceptibility data indicates linear region in high temperature region corresponding to PM phase followed by the downturns confirming the presence of Griffith phase in pristine and Ce doped $TbMnO_3$ systems.

M-H curve of $TbMnO_3$, $Tb_{0.975}Ce_{0.025}MnO_3$ and $Tb_{0.95}Ce_{0.05}MnO_3$ at T = 5 K under field cooling FC (0 kOe, 10 kOe, 20kOe, 30 kOe) is shown in Fig. 7(a, b and c) which show straight line nature of pure antiferromagnetic material. Interestingly, the isothermal magnetization data at 5 K under zero field cooling condition for $TbMnO_3$ indicates a metamagnetic transition at 1.7 T (inset of Fig. 2), which can be attributed to the magnetic reversal of Ising Tb^{3+} moments, as previously observed in both polycrystalline and single crystal $TbMnO_3$ [3,39]. From Fig. 6 it is clear that on increasing FC (field cooling) coercivity of M-H loop increases and also origin of hysteresis loop is shifted. This shows that conventional exchange bias phenomena in $TbMnO_3$ system exist as found in bilayers or multilayer magnetic systems and thin film [40]. All the samples show conventional exchange bias. $TbMnO_3$ and $Tb_{0.95}Ce_{0.05}MnO_3$ show similar shift (~60 Oe) in the H axis whereas the shift in $Tb_{0.975}Ce_{0.025}MnO_3$ (~20 Oe) is less than that in those two samples while the samples were cooled in presence of 30 kOe cooling field. Interestingly, from the structural study, it has been found that $TbMnO_3$ and $Tb_{0.95}Ce_{0.05}MnO_3$ shows larger deviation of the lattice parameter (Mn-O-Mn angle) due to JT distortion. It is well known that exchange bias effect is attributed to inhomogeneous magnetic ordering in magnetic materials e.g. multilayer of AFM and FM. However,

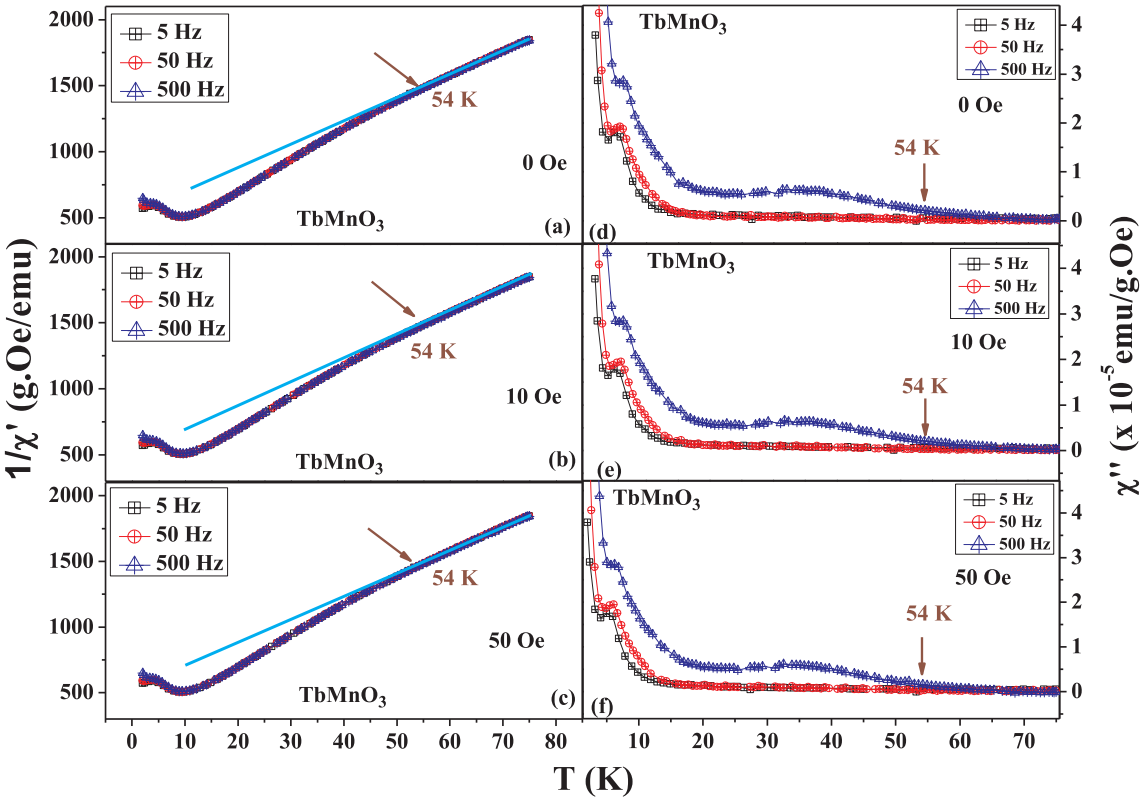

Fig. 4. Inverse of real part of AC susceptibility (1/χ') measured at different applied dc fields (a) 0 Oe (b) 10 Oe and (c) 50 Oe and imaginary part of AC susceptibility of $TbMnO_3$ at (d) 0 Oe (e) 10 Oe and (f) 50Oe.

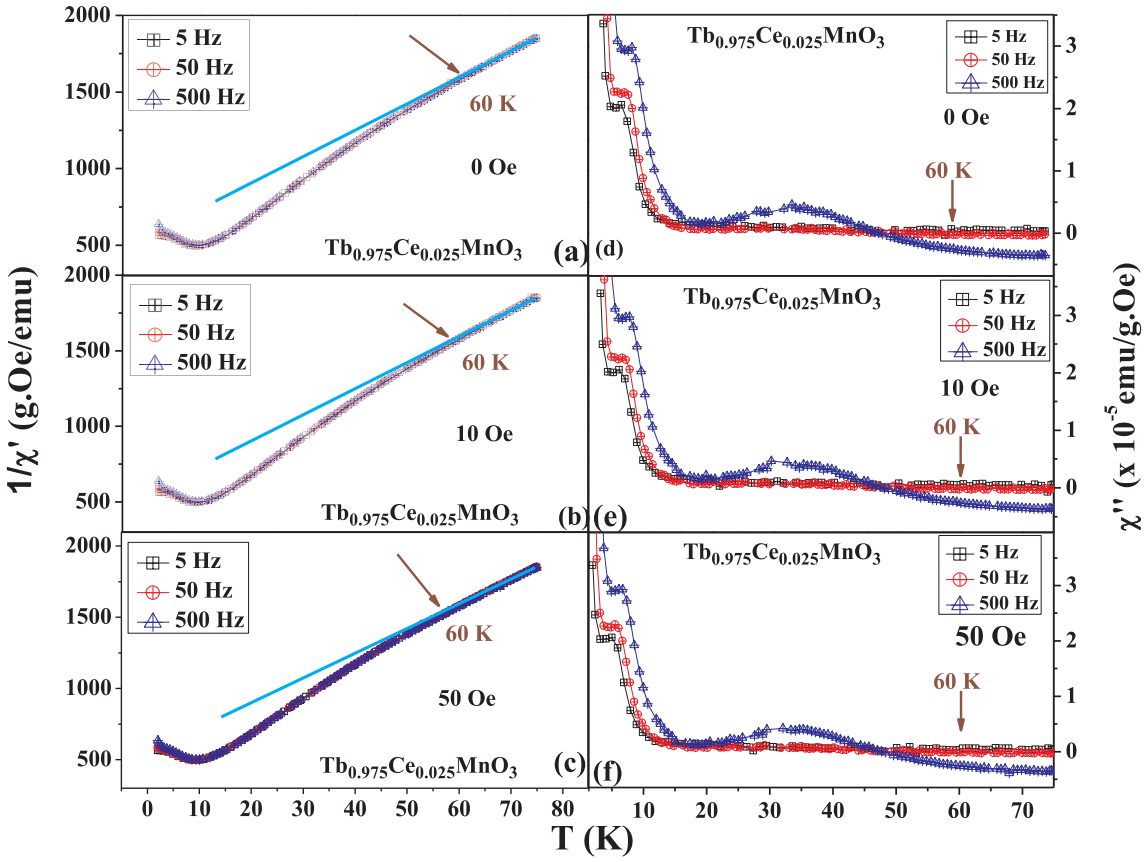

Fig. 5. Inverse of real part of AC susceptibility ($1/\chi'$) measured at different applied dc fields (a) 0 Oe (b) 10 Oe and (c) 50Oe and imaginary part of AC susceptibility (χ'') of $Tb_{0.975}Ce_{0.025}MnO_3$ at (d) 0 Oe (e) 10 Oe and (f) 50Oe).

$TbMnO_3$ is known to show antiferromagnetic ordering at temperature below ~ 40 K. Thus, the origin of the weak ferromagnetic behaviour cannot be understood simply. It is worthy to mention here that from the XRD results we have seen that Jahn-Teller distortion exists in the system, which could induce the canted antiferromagnetic ordering. Canted antiferromagnetism (Canted AFM) is a particular arrangement of spin in which the spins aligned antiferromagnetically are not perfectly antiparallel to each other. Rather they make an acute angle to each other. As a result, there happens to be a net magnetization in a particular direction. The weak ferromagnetism thus can be interpreted in terms of the Dzyaloshinskii-Moriya interaction [1], which happens to be an intrinsic feature of the canted anitiferromagnetism. As we know from the definition of DM interaction, it is dependent on the angle between the interacting spins. The Hamiltonian term for DM interaction can be written as, $H_{DM} = D_{ij}.(S_i \times S_j)$ where Si and Sj are the two interacting spin moments. Hence, if the ferromagnetic moment in an antiferromagnetic material increases due to the spin canting the exchange bias will also increase.

In the present investigation it may be suggested that the oxygen vacancy may be the origin of ferromagnetism which in effect leads to the Griffith phase and exchange bias. To verify this prediction, we have recorded the X-ray photoelectron spectra at Mn2*p* and O1*s* edge of $TbMnO_3$ and $Tb_{0.95}Ce_{0.05}MnO_3$. X-ray photoelectron spectroscopy (XPS) is one of the most used surface sensitive techniques to study the valence states of any element in a material. The core level XPS spectra at Mn2*p* and O1*s* edge of the sample $TbMnO_3$ [Fig. 8(a and b)] and $Tb_{0.95}Ce_{0.05}MnO_3$, [Fig. 8(c and d)] were recorded at room temperature which are presented in Fig. 8. The Mn2*p* peaks are split into two regions corresponding to $2p_{3/2}$ and $2p_{1/2}$ levels at binding energy ~652.9 and 641.2 eV due to spin orbit coupling. Both the peaks ($2p_{3/2}$ and $2p_{1/2}$) are asymmetric in nature indicating the presence of mixed valence of Mn in both the samples. After a background correction (Shirley) the peaks were deconvoluted into two peaks corresponding to Mn^{3+} and Mn^{2+}. The peaks at ~641.8 and 642.7 eV and peaks ~653.3 and 653.6 eV in Fig. 8a and c correspond to the Mn^{3+} phase in $2p_{3/2}$ and $2p_{1/2}$ spectra of $TbMnO_3$ and $Tb_{0.95}Ce_{0.05}MnO_3$ respectively [30,31]. Whereas the peaks ~640.8 and 640.7 eV and peaks ~651.7 and 652.2 eV in Fig. 8a and c correspond to the Mn^{2+} phase in $2p_{3/2}$ and $2p_{1/2}$ spectra of $TbMnO_3$ and $Tb_{0.95}Ce_{0.05}MnO_3$ respectively [41,42]. The relative amount of Mn^{2+} between the Mn ions, calculated using the area under the peak in the parent and doped compound were 21.5% and 32.4%. Presence of 2+ state in addition to the expected 3+ state of Mn ions have previously been observed in $TbMnO_3$ thin films by Rubi et al., [21]. In many perovskite manganite the mixed valence state have been found and were explained to arise in the system due to the oxygen vacancy present in the system. To balance the charge imbalance created by doping of Ce^{4+} ions in the system some Mn^{3+} ions gets converted to Mn^{2+} ions. Thus, larger amount of Mn^{2+} can be found in the Ce doped sample.

In Fig. b and d the O1*s* core level XPS spectra of $TbMnO_3$ and $Tb_{0.95}Ce_{0.05}MnO_3$ are presented which are split into two parts revealing two kinds of chemical state of oxygen to be present in the compounds. The peaks at binding energy position ~528.9 eV correspond to the oxygen situated at lattice denoted as O_L and the peak positioned at ~531.4 eV corresponds to the surface chemisorbed oxygen denoted by O_V. The surface chemisorption of the of oxygen ions occurs due to the presence of oxygen vacancy in the system. In manganite systems it is common to find the oxygen vacancies which are created at the surface due to lattice defects [41–43].

Existence of the mixed Mn^{2+}/Mn^{3+} states may induce ferromagnetism [19]. We have also doped Ce in the Tb site of $TbMnO_3$ and synthesized $Tb_{0.975}Ce_{0.025}MnO_3$ and $Tb_{0.95}Ce_{0.05}MnO_3$ samples. The

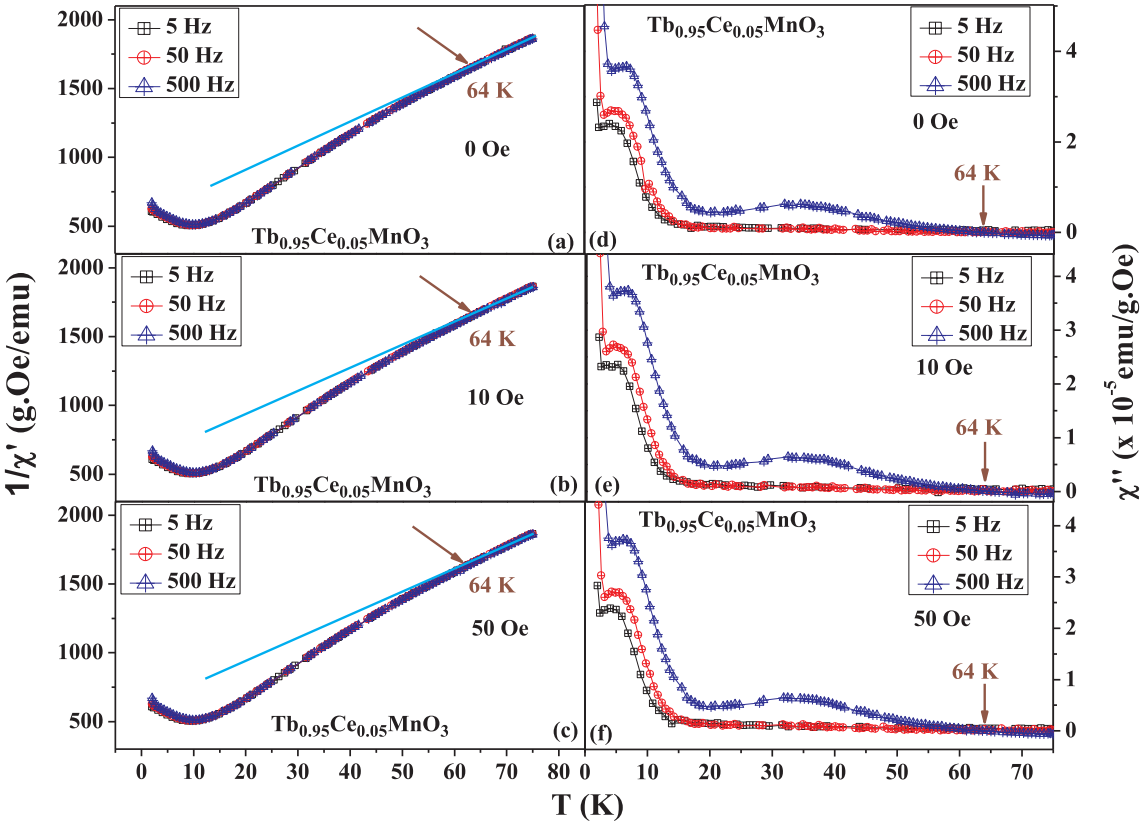

Fig. 6. Inverse of real part of AC susceptibility ($1/\chi'$) measured at different applied dc fields (a) 0 Oe (b) 10 Oe and (c) 50 Oe and imaginary part of AC susceptibility (χ'') of $Tb_{0.95}Ce_{0.05}MnO_3$ (d) 0 Oe (e) 10 Oe and (f) 50Oe.

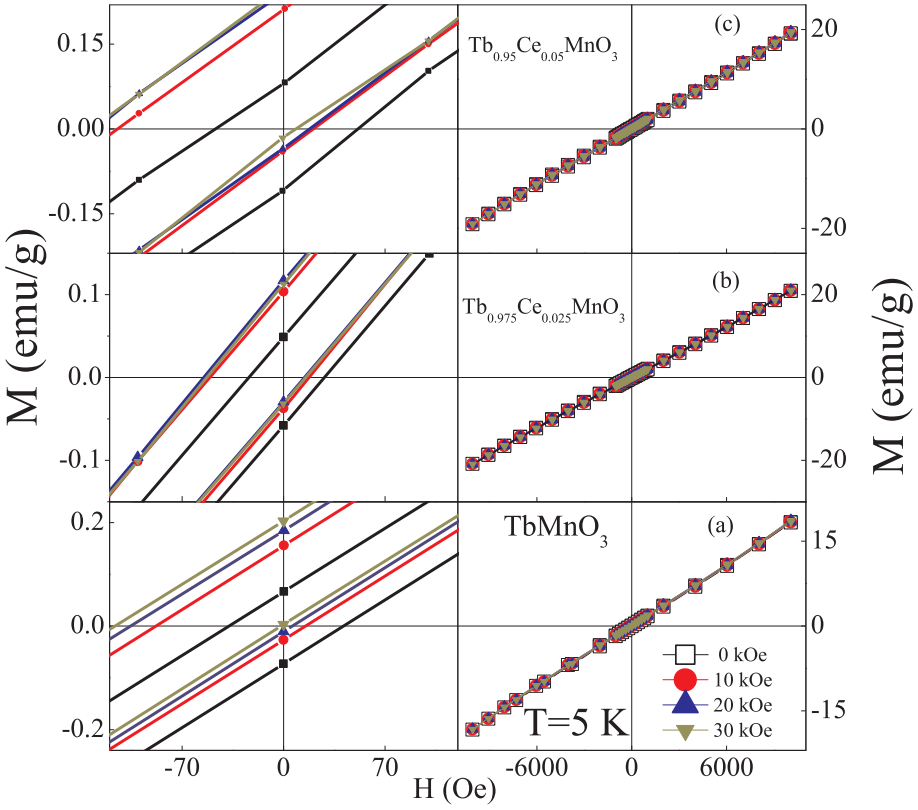

Fig. 7. (a, b, c) M-H curve of $TbMnO_3$, $Tb_{0.975}Ce_{0.025}MnO_3$, $Tb_{0.95}Ce_{0.05}MnO_3$ respectively at 5 K and (d, e, f) indicate extended view of these figures clearly indicating presence of exchange bias.

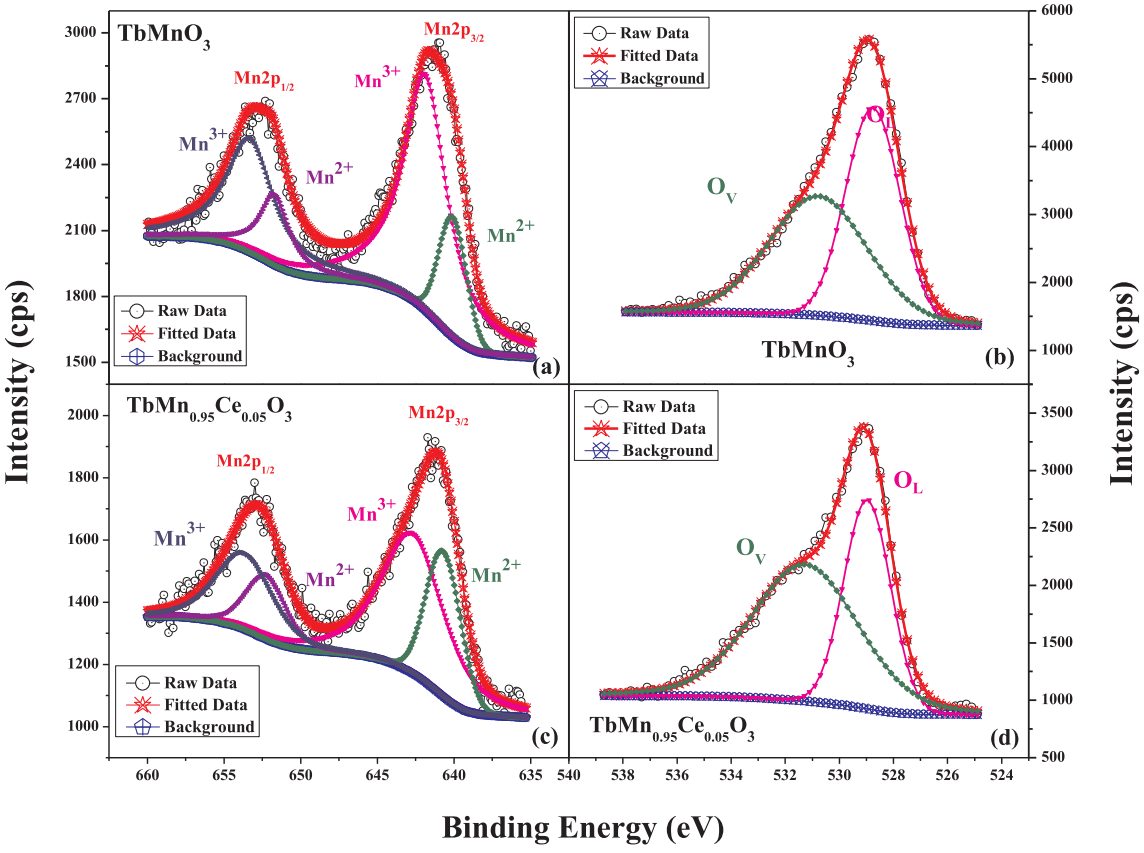

Fig. 8. The core level XPS spectra at Mn2*p* and O1*s* edge of the sample $TbMnO_3$ (a and b) and $Tb_{0.95}Ce_{0.05}MnO_3$, (c and d).

enhancement in exchange bias and the Griffith's phase behavior of these samples (shown in Figs. 2–7) supports our assumptions that Mn lies in two different valence state. Ce doping in $TbMnO_3$, which exists in the tetravalent (Ce^{4+}) state, might be driving some of the Mn^{3+} ions into a Mn^{2+} state [41]. Exchange interaction between Mn^{3+} and Mn^{2+} is inducing ferromagnetism in $TbMnO_3$ which might be the origin of Griffith phase observed in $TbMnO_3$ and Ce doped $TbMnO_3$. In addition to that, strong orthorhombic disorder is common phenomenon in rare earth perovskite material due to the presence of A-site disorder which is expected to enhance upon doping of small amount of Ce^{4+} due to the difference in ionic radii of Ce and Tb. Moreover, Mn^{3+} ion is known to be Jahn-Teller (JT) distortion active which can bring a strong local JT distortion in the lattice [42]. Thus, the large change in the Mn–O–Mn bond angle can be attributed to the JT distortion through the tilting of MnO_6 octahedra. As evident from the structural data that all the samples satisfy the condition for JT distortion [b > a > c/√2] condition, it can be concluded that the JT distortion plays vital role in determining the properties of the system [44]. Doping of Ce ion initially reduces the distortion as it effectively decreases the amount of JT active Mn^{3+}. Some of the Mn^{3+} ions are converted to Mn^{2+} to maintain the charge neutrality. But, with further increasing the doping level the distortion increases as the lattice strain is expected increase due to the difference between the ionic radii of Tb and Ce. The magnetic properties are bound to change due to this orthorhombic distortion as it causes Mn ions to orient from its initial position which in turn can cause different magnetic interactions in the lattice. The double exchange interaction between Mn^{3+} and Mn^{2+} is known to be ferromagnetic whereas super exchange interaction Mn^{3+} and Mn^{3+} is antiferromagnetic [41]. Moreover, the presence of different valence state of Mn ions (Mn^{3+} and Mn^{2+}) and the orientation of Mn ions creates weak ferromagnetic clusters and the canted antiferromagnetic ordering in the system. The change in Mn–O–Mn induces the canted anti-ferromagnetic orderingin $TbMnO_3$ [39]. Thus the exchange bias increases due to increase in the canted antiferromagnetic ordering.

4. Conclusion

In summary, we have investigated the magnetic properties of $Tb_{1-x}Ce_xMnO_3$ (x = 0.0, 0.025, 0.05). The pure and doped sample showed the existence of both exchange bias and Griffith phase. The Griffith phase has been attributed to the oxygen vacancy which converts some Mn^{3+} states to Mn^{2+} states. The possibility of Jahn–Teller distortion due the presence of Mn^{3+} ions has been discussed which significantly changes the Mn–O–Mn angle. This, in turn, creates canted antiferromagnetic ordering which might be responsible for getting the exchange bias in the system. The exchange interaction between Mn^{3+}/Mn^{2+} induces ferromagnetism. Furthermore, Ce doping also converts some Mn^{3+} states to Mn^{2+} states. As a consequence, Ce doped $TbMnO_3$ also show Griffith phase. Moreover, The Oxygen vacancy and J-T diostortion ions may change the Mn–O–Mn angle which in effect enhances the canted AFM ordering.

Declaration of Competing Interest

The authors declare that they have no known competing financial interests or personal relationships that could have appeared to influence the work reported in this paper.

Acknowledgement

Authors would like to acknowledge the central instrument facility centre of IIT (BHU) for and magnetic measurements.

Appendix A. Supplementary data

Supplementary data to this article can be found online at https://

doi.org/10.1016/j.jmmm.2019.166261.

References

[1] S.-W. Cheong, M. Mostovoy, Nature Mater. 6 (2007) 13.
[2] M. Pekala, V. Drozd, J.F. Fagnard, P. Vanderbemden, M. Ausloos, J. All. Comp. 467 (2009) 35–40.
[3] T. Kimura, T. Goto, H. Shintani, K. Ishizaka, T. Arima, Y. Tokura, Nature 426b (2003) 55–58.
[4] T. Goto, T. Kimura, G. Lawes, A.P. Ramirez, Y. Tokura, Phys. Rev. Lett. 92 (2004) 257201.
[5] B. Lorenz, Y.Q. Wang, C.-W. Chu, Phys. Rev. B 76 (2007) 104405.
[6] H.D. Zhou, J.C. Denyszyn, J.B. Goodenough, Phys. Rev. B 72 (2005) 224401.
[7] O. Prokhnenko, R. Feyerherm, M. Mostovoy, N. Aliouane, E. Dudzik, A.U.B. Wolter, A. Maljuk, D.N. Argyriou, Phys. Rev. Lett. 99 (2007) 177206.
[8] Y.Y. Guo, Y.J. Guo, N. Zhang, L. Lin, J.M. Liu, Appl. Phys. A 106 (2012) 113.
[9] P. Rovillain, M. Cazayous, Y. Gallais, A. Sacuto, M.A. Measson, H. Sakata, Phys. Rev. B 81 (2010) 054428.
[10] F.W. Fabris, M. Pekala, V. Drozd, J.F. Fagnard, P. Vanderbemden, R.S. Liu, M. Ausloos, J. Appl. Phys. 101 (2007) 103904.
[11] J. Blasco, C. Ritter, J. Gorcia, J.M. de-Teresa, J. Perez-Cacho, M.R. Ibarra, Phys. Rev. B 62 (2000) 5609.
[12] T. Goto, Y. Yamasaki, H. Watanabe, T. Kimura, Y. Tokura, Phys. Rev. B 72 (2005) 220403.
[13] N. Mufti, A.A. Nugoroho, G.R. Blake, T.T.M. Palstra, Phys. Rev. B 78 (2008) 024109.
[14] D.O. Flynn, C.V. Tomy, M.R. Lees, A. Daoud-Aladin, G. Balakrishnan, Phys. Rev. B 83 (2011) 174426.
[15] M. Mostovoy, Phys. Rev. Lett. 96 (2006) 067601.
[16] O. Prokhnenko, N. Aliouane, R. Feyerherm, E. Dudzik, A.U.B. Wolter, A. Maljuk, K. Kiefer, D.N. Argyriou, Phys. Rev. B 81 (2010) 024419.
[17] W.H. Meiklejohn, C.P. Bean, Phys. Rev. 105 (1957) 904.
[18] A.E. Berkowitz, K. Takano, J. Magn. Magn. Mater. 200 (1999) 552.
[19] R.B. Griffiths, Phys. Rev. Lett. 23 (1969) 17.
[20] C. Magen, P.A. Algarabel, L. Morellon, J.P. Araujo, C. Ritter, M.R. Ibarra, A.M. Pereira, J.B. Sousa, Phys. Rev. Lett. 96 (2006) 167201.
[21] D. Rubi, C. de Graaf, C.J.M. Daumont, D. Mannix, R. Broer, B. Noheda, Phys. Rev. B 79 (2009) 014416.
[22] D. O'Flynn, M.R. Lees, G. Balakrishnan, J. Phys.: Condens. Matter 26 (2014) 256002.
[23] A. Kumar, G.D. Dwivedi, A. Singh, R. Singh, K.K. Shukla, H.D. Yang, A.K. Ghosh, S. Chatterjee, AIP Conf. Proc. 1731 (2015) 130060.
[24] R.D. Shanon, Acta Crysta. A 32 (1976) 751.
[25] A. Paul, S. Mattauch, Appl. Phys. Lett. 95 (2009) 092502.
[26] S.M. Zhou, S.Y. Zhao, Y.Q. Guo, J.Y. Zhao, L. Shi, J. Appl. Phys. 107 (2010) 033906.
[27] T.W. Eom, Y.H. Hyun, J.S. Park, Y.P. Lee, V.G. Prokhorov, V.S. Flis, V.L. Svetchnikov, Appl. Phys. Lett. 94 (2009) 152502.
[28] V.N. Krivoruchko, Low Temp. Phys. 40 (2014) 586.
[29] J. Deisenhofer, D. Braak, H.-A. Krug von Nidda, J. Hemberger, R.M. Eremina, V.A. Ivanshin, A.M. Balbashov, G. Jug, A. Loid, T. Kimura, Y. Tokura, Phys. Rev. Lett. 95 (2005) 257202.
[30] A. Karmakar, S. Majumdar, S. Kundu, T.K. Nath, S. Giri, J. Phys.: Condens. Matter 25 (2013) 066006.
[31] C. Magen, P.A. Algarabel, L. Morellon, J.P. Araujo, C. Ritter, M.R. Ibarra, A.M. Pereira, J.B. Sousa, Phys. Rev. Lett. 96 (2006) 167201.
[32] M.B. Salamon, P. Lin, S.H. Chun, Phys. Rev. Lett. 88 (2002) 197203.
[33] R. Venkatesh, M. Pattabiraman, S. Angappane, G. Rangarajan, K. Sethupathi, J. Karatha, M.F. Morariu, R.M. Ghadimi, G. Guntherodt, Phys. Rev. B 75 (27) 224415.
[34] A.K. Pramanik, A. Banerjee, J. Phys.: Condens. Matter 28 (2016) 35LT02.
[35] Z.W. Ouyang, V.K. Pecharsky, K.A. Gschneidner, D.L. Schlagel Jr., T.A. Lograsso, Phys. Rev. B 74 (2006) 094404.
[36] P. Tong, B. Kim, D. Kwon, T. Qian, S.-I. Lee, S.-W. Cheong, B.G. Kim, Phys. Rev. B 77 (2008) 184432.
[37] J.H. Albillos, L.M. Garcıa, F. Bartolome, J. Phys.: Condens. Matter 21 (2009) 21600.
[38] Z.W. Ouyang, J. Appl. Phys. 108 (2010) 033907.
[39] M. Staruch, G. Lawes, A. Kumarasiri, L.F. Cotica, M. Jain, Appl. Phys. Lett. 102 (2013) 062908.
[40] X. Martí, F. Sánchez, D. Hrabovsky, L. Fàbrega, A. Ruyter, J. Fontcuberta, V. Laukhin, V. Skumryev, M.V. García-Cuenca, C. Ferrater, M. Varela, A. Vilà, U. Lüders, J.F. Bobo, Appl. Phys. Lett. 89 (2006) 032510.
[41] G.D. Dwivedi, A. Kumar, K.S. Yang, B.Y. Chen, K.W. Liu, S. Chatterjee, H.D. Yang, H. Chou, Appl. Phys. Lett. 108 (2016) 192409.
[42] A. Pal, S. Ghosh, A.G. Joshi, S. Kumar, S. Patil, P.K. Gupta, P. Singh, V.K. Gangwar, P. Prakash, R.K. Singh, E.F. Schwier, M. Sawada, K. Shimada, A.K. Ghosh, A. Das, S. Chatterjee, J. Phys.: Condens. Matter 31 (2019) 275802.
[43] P. Raychaudhuri, S. Mukherjee, A.K. Nigam, J. John, U.D. Vaisnav, R. Pinto, P. Mandal, J. Appl. Phys. 86 (1999) 5718.
[44] J.A. Alonso, M.J. Martınez-Lope, M.T. Casais, M.T. Fernandez-Dıaz, Inorg. Chem. 39 (2000) 917.